ARL-TR-10102 ● MAY 2025

Post–Focused Ion Beam (FIB) Transmission Electron Microscopy (TEM) Sample Processing: Low-Angle Ion Mill Cleanup

by Wendy L. Sarney, Xiaohang Zhang, Mihee Ji, and Asher C. Leff

NOTICES

Disclaimers

The findings in this report are not to be construed as an official Department of the Army position unless so designated by other authorized documents.

Citation of manufacturer's or trade names does not constitute an official endorsement or approval of the use thereof.

Destroy this report when it is no longer needed. Do not return it to the originator.

ARL-TR-10102 ● MAY 2025

Post–Focused Ion Beam (FIB) Transmission Electron Microscopy (TEM) Sample Processing: Low-Angle Ion Mill Cleanup

Wendy L. Sarney and Mihee Ji
DEVCOM Army Research Laboratory

Xiaohang Zhang
General Technical Services

Asher C. Leff
TauMat Tech

REPORT DOCUMENTATION PAGE

1. REPORT DATE	2. REPORT TYPE	3. DATES COVERED	
		START DATE	END DATE
May 2025	Technical Report	1/01/2023	4/23/2025

4. TITLE AND SUBTITLE
Post–Focused Ion Beam (FIB) Transmission Electron Microscopy (TEM) Sample Processing: Low-Angle Ion Mill Cleanup

5a. CONTRACT NUMBER	5b. GRANT NUMBER	5c. PROGRAM ELEMENT NUMBER
5d. PROJECT NUMBER	**5e. TASK NUMBER**	**5f. WORK UNIT NUMBER**

6. AUTHOR(S)
Wendy L. Sarney, Xiaohang Zhang, Mihee Ji, and Asher C. Leff

7. PERFORMING ORGANIZATION NAME(S) AND ADDRESS(ES)	8. PERFORMING ORGANIZATION REPORT NUMBER
DEVCOM Army Research Laboratory ATTN: FCDD-RLA-PE Adelphi, MD 20783	ARL-TR-10102

9. SPONSORING/MONITORING AGENCY NAME(S) AND ADDRESS(ES)	10. SPONSOR/MONITOR'S ACRONYM(S)	11. SPONSOR/MONITOR'S REPORT NUMBER(S)

12. DISTRIBUTION/AVAILABILITY STATEMENT
DISTRIBUTION STATEMENT A. Approved for public release: distribution unlimited.

13. SUPPLEMENTARY NOTES
ORCIDs: Wendy L. Sarney, 0000-0003-4024-1186; Asher C. Leff, 0000–0002–2226–9014; Mihee Ji 0000-0002-8160-6463; Xiaohang Zhang 0000-0001-5395-0235

14. ABSTRACT
Focused ion beam (FIB) milling is a widely used technique for preparing thin lamellae for transmission electron microscopy. While FIB can yield foils with sufficient electron transparency, challenges remain in achieving optimal final thickness due to limitations in low-energy imaging and the need to preserve protective surface layers. Incomplete thinning, gallium ion (Ga^+) damage, and post-milling oxidation can degrade image quality. To address these issues, a post-FIB treatment using low-energy, low-angle argon ion milling is employed in a Gatan precision ion polishing system. This report outlines the alignment and milling procedures, emphasizing careful control of milling angle and time to avoid removal of the protective platinum/carbon cap layers. Examples demonstrate enhanced image clarity and improved high-resolution lattice imaging in hafnium zirconium oxide and aluminum gallium nitride/aluminum nitride samples after post-FIB ion milling.

15. SUBJECT TERMS
focused ion beam; transmission electron microscopy; microanalysis; sample preparation; Photonics, Electronics, and Quantum Sciences; PE&QS; Electromagnetic Spectrum Sciences; EMSS

16. SECURITY CLASSIFICATION OF:			17. LIMITATION OF ABSTRACT	18. NUMBER OF PAGES
a. REPORT	b. ABSTRACT	C. THIS PAGE		
UNCLASSIFIED	UNCLASSIFIED	UNCLASSIFIED	UU	21

19a. NAME OF RESPONSIBLE PERSON	19b. PHONE NUMBER *(Include area code)*
Wendy L. Sarney	(520) 691-5146

STANDARD FORM 298 (REV. 5/2020)
Prescribed by ANSI Std. Z39.18

Contents

List of Figures

1. Introduction

Cross-sectional films must be less than 100 nm thick for transmission electron microscopy (TEM) analysis, and high-resolution atomic scale imaging requires even thinner lamellae. Focused ion beam (FIB) preparation typically yields thin foils with large electron-transparent areas.

Assessing sufficient thinning within the FIB is challenging, in part due to the low energies used for imaging in the final stages and the tendency to avoid imaging as the sample reaches electron transparency. Because of this, it can be difficult to precisely know the sample thickness. Consequently, FIB milling is often prematurely terminated. Softer materials are especially susceptible to this issue due to their faster milling rates.

Even at low milling angles and energies, samples can have some degree of ion (i^+) beam-related damage or even unwanted gallium ion (Ga^+) incorporation. Samples can oxidize during transport between the FIB, TEM, and storage.[1] TEM imaging can often be greatly improved with a small amount of post-FIB thinning in the Gatan precision ion polishing system (PIPS).[2]

In this report, we detail our procedure for post-FIB low-angle cleanup in the PIPS. We use detailed schematics to describe the configuration of the sample and the beams in the PIPS, and show TEM and scanning transmission electron microscopy (STEM) images taken before and after cleanup.

1.1 Challenges Related to the Final FIB Thinning of TEM Samples

The geometry of the i^+ and electron (e^-) beams relative to the sample in the Thermo Scientific Helios G4 UX DualBeam system is described in a prior report.[3] The beams have fixed positions, but the sample can be tilted as needed for i^+ and e^- beam imaging and deposition, along with i^+ beam milling (Figure 1). When the sample is at its zero position, the e^- beam is normal to its surface, and the i^+ beam is 52° from the e^- beam (Figure 1a). From this position, the cross-sectional thickness of the sample (orange arrows) is visible along the eventual TEM beam direction (Figure 1b). The i^+ beam image (Figure 1c) shows an inclined view of one of the cross-sectional faces.

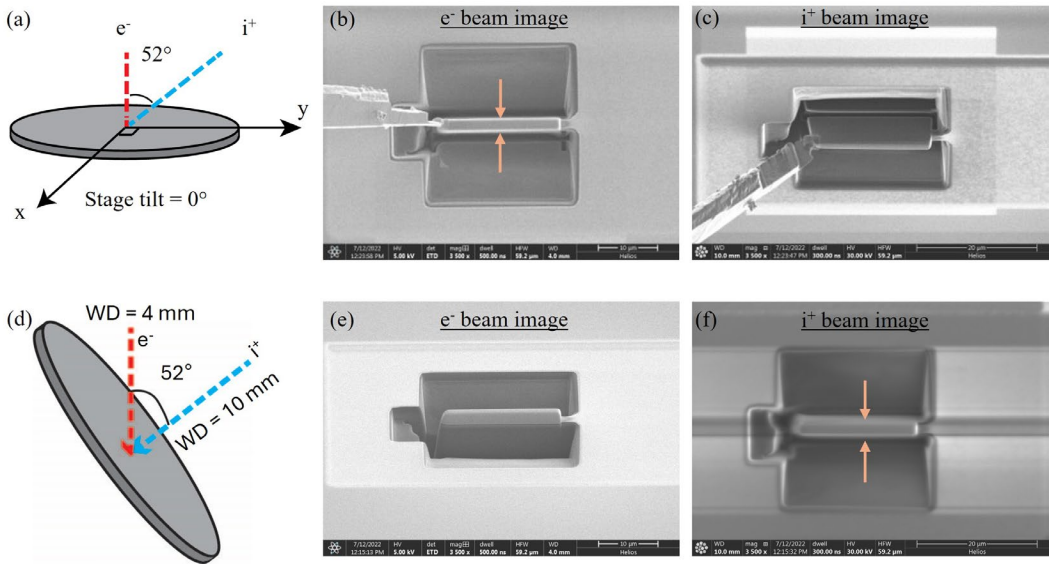

Figure 1. Arrangement of sample inside FIB (a) when oriented at 0° tilt with corresponding (b) e- and (c) i+ beam images. Arrangement of sample (d) when oriented towards i+ beam with corresponding (e) e^- and (f) i^+ beam images. Cross-sectional thickness is denoted with orange arrows.

If the sample is positioned to face the i^+ beam (Figure 1d), the e^- beam view shows the inclined face opposite of that visible in Figure 1c. The i^+ beam image (Figure 1f) shows the cross-sectional thickness. During milling, the sample is positioned at 53.7° (with the i^+ beam incident at 1.7° to the sample face). The e^- beam image does not show the sample thickness unless you intermittently stop the thinning and tilt the sample so that its surface is normal to the e^- beam. The images collected in Figure 1 are for samples that are still very thick, and the i^+ beam energy is 30 keV, which is much higher than it will be in the last stages (5 and 2 keV).

Although the sample thickness can be seen in the i^+ beam image when it is in the milling position, images need to be minimized to reduce beam damage. Furthermore, the end stages use such low i^+ beam energies that the images are unclear, especially when the sample gets very thin. Figure 2 shows the (a) e^- and (b) i^+ image when the sample is nearing the last stages. The i^+ beam image was collected at 2 keV. The image is not crisp because we can only make limited corrections to focus and stigmation to minimize beam exposure.

Milling must be stopped before the overlying platinum (Pt) or carbon (C) protective layer is completely removed. Without the protective layer, we cannot be sure that we are imaging the normal of the sample's true surface, precluding accurate layer thickness measurements and surface profiling in the TEM. Often, the surface layers are extremely thin (less than 1 nm); therefore, if the protective layer is milled away, the region of interest may also be lost.

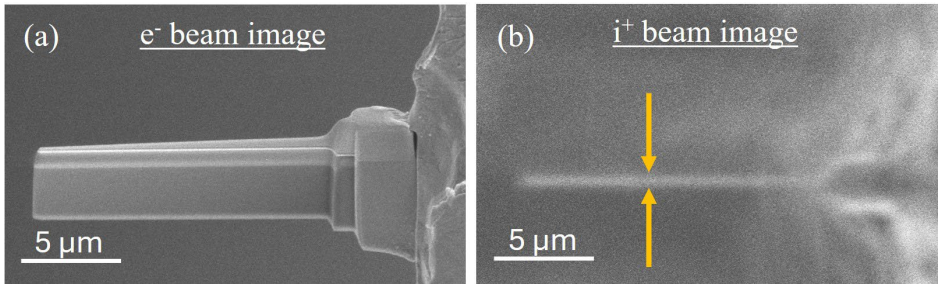

Figure 2. (a) e- and (b) i+ beam images before final thinning at 2 keV. We avoid imaging at this late state of sample preparation to minimize beam damage.

1.2 Low-Energy, Low-Angle Ion Beam Cleanup

The PIPS uses argon ion (Ar^+) beams, whereas the FIB uses Ga^+ beams. Argon, being a noble gas, is chemically inert. Gallium (Ga) has a heavier mass (69 amu vs. 40 amu).[4] This greater mass results in higher momentum during collisions with the sample, leading to increased sputtering and greater potential for sample damage. Ga^+ penetrate deeper into the lamellae and can cause subsurface damage and Ga implantation. A 30-keV ion beam can induce damage up to 20–30 nm deep, typically manifesting as amorphization.[5]

2. Low-Angle Ion Milling Procedure for FIB Samples

Prior to sample loading, align the left-hand (LH) and right-hand (RH) beams using the fluorescent screen. Remove the screen and allow the PIPS to operate until the beams are stable at 0.5 keV.

The TEM sample, mounted on its FIB grid, is secured in the PIPS clamping post, as illustrated in Figure 3.

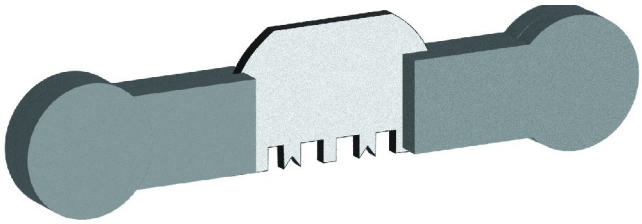

Figure 3. FIB grid inside Gatan DuoPost.

The DuoPost clamp is then positioned as depicted in Figure 4, ensuring the grid teeth face the front of the PIPS.

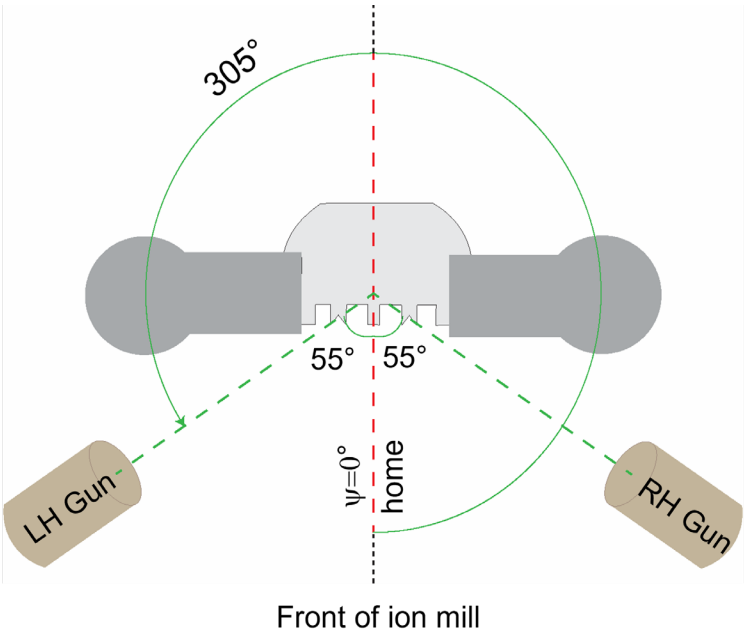

Figure 4. Arrangement of DuoPost in the PIPS (top-down view).

The RH and LH i^+ guns are positioned 110° apart. The clamping post's home position is defined by aligning the normal to its horizontal axis (red dashed line) with the center of the PIPS. If that is not true, calibrate the home position as described in the manual. The angles displayed in the Alignment menu (Figure 5) on the PIPS correlate to the physical positions of the guns as shown in Figure 4.

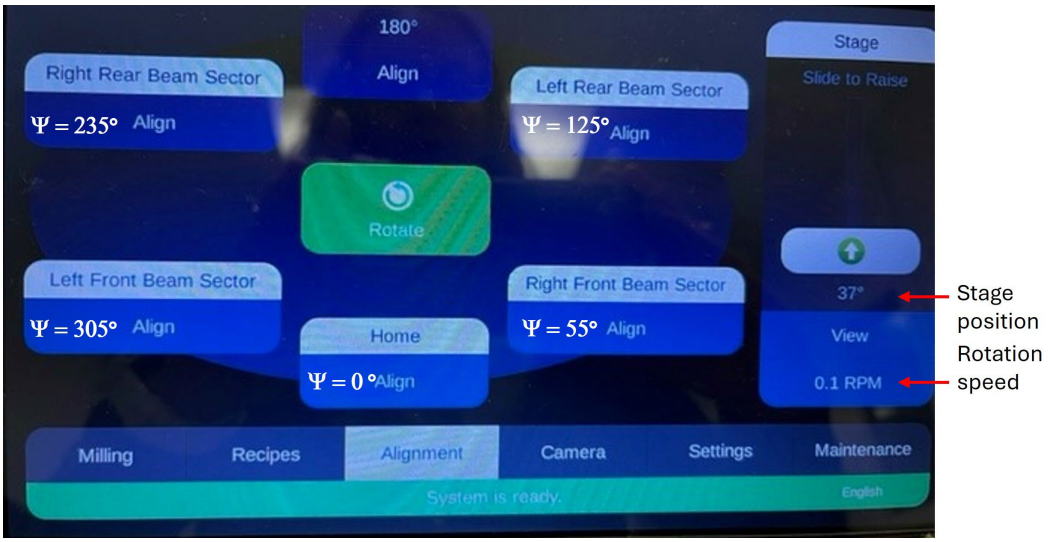

Figure 5. Alignment window on PIPS front panel.

We define the reference angle Ψ = 0° as shown in Figure 4. Consequently, the RH and LH i^+ guns are positioned at 55° and 305°, respectively, measured counterclockwise from the center axis of the PIPS (the black dashed line in

Figure 4). When selecting either the right or left beam sector (Figure 5), the corresponding angle positions are 55° and 305°. The "Rotate" button illuminates green when the sample is actively rotating.

We use either the RH or LH gun, prioritizing the one exhibiting greater stability at low kiloelectron volts. The gun is selected under the Milling-Modulation menu. Stationary Right means that the RH gun is on continuously, the LH gun is off, and the sample does not rotate. Similarly, Stationary Left means that the LH gun is on continuously, the RH gun is off, and the sample does not rotate. Based on the selected gun and the sample's orientation on the grid, we choose one of the two front beam sector arrangements to ensure the DuoPost's main axis is normal to the beam. We then reduce the rotation speed to 0.5–0.1 rpm and move the sample to its final position, as detailed in the following paragraphs and figures.

To prevent milling of the specimen grid and subsequent redeposition onto the sample, we offset the sample 5° from direct beam incidence. The precise orientations are illustrated in Figures 6–9. Figure 6a depicts the position within the PIPS chamber, with Figure 6b providing an enlarged view and Figure 6c presenting a different perspective.

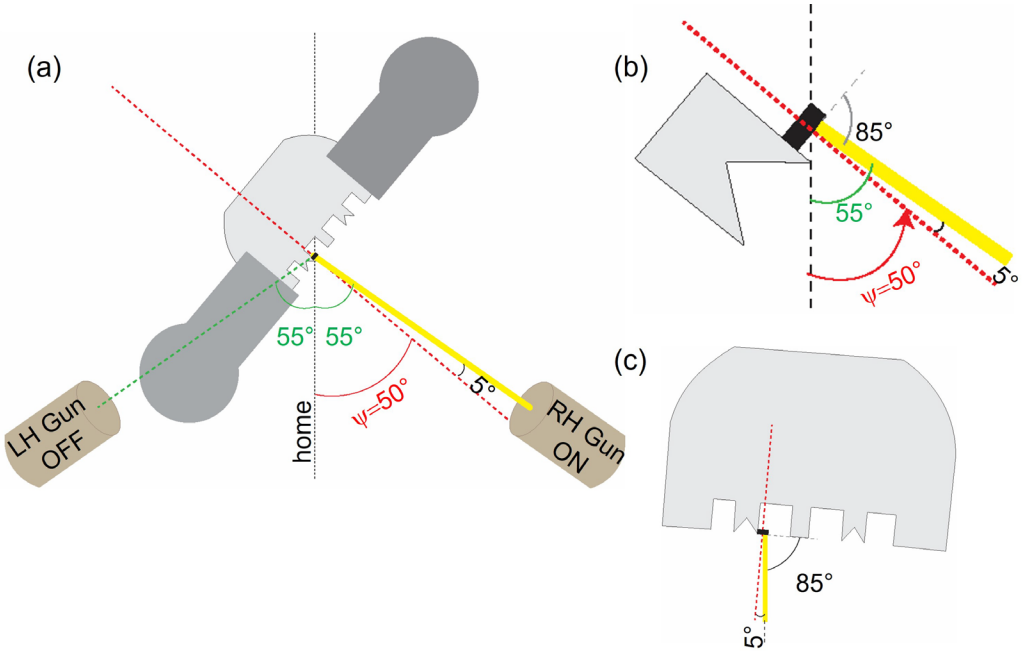

Figure 6. Configuration for using the RH gun, sample mounted on right-side face of grid tooth (from perspective of teeth facing down).

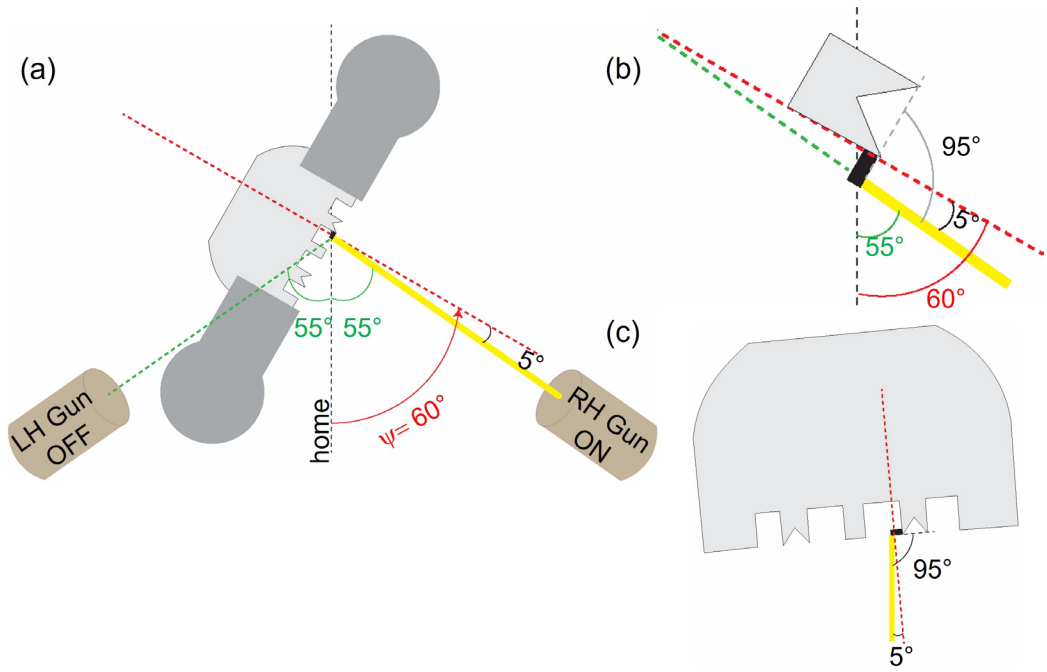

Figure 7. Configuration for using the RH gun, sample mounted on left-side face of grid tooth (from perspective of teeth facing down).

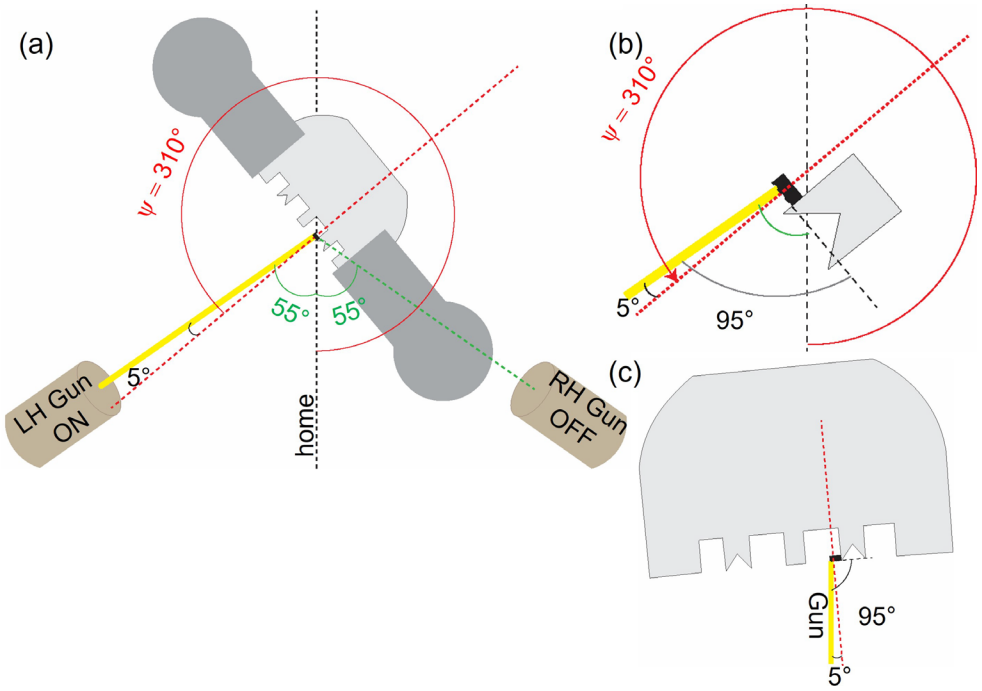

Figure 8. Configuration for using the LH gun, sample mounted on left-side face of grid tooth (from perspective of teeth facing down).

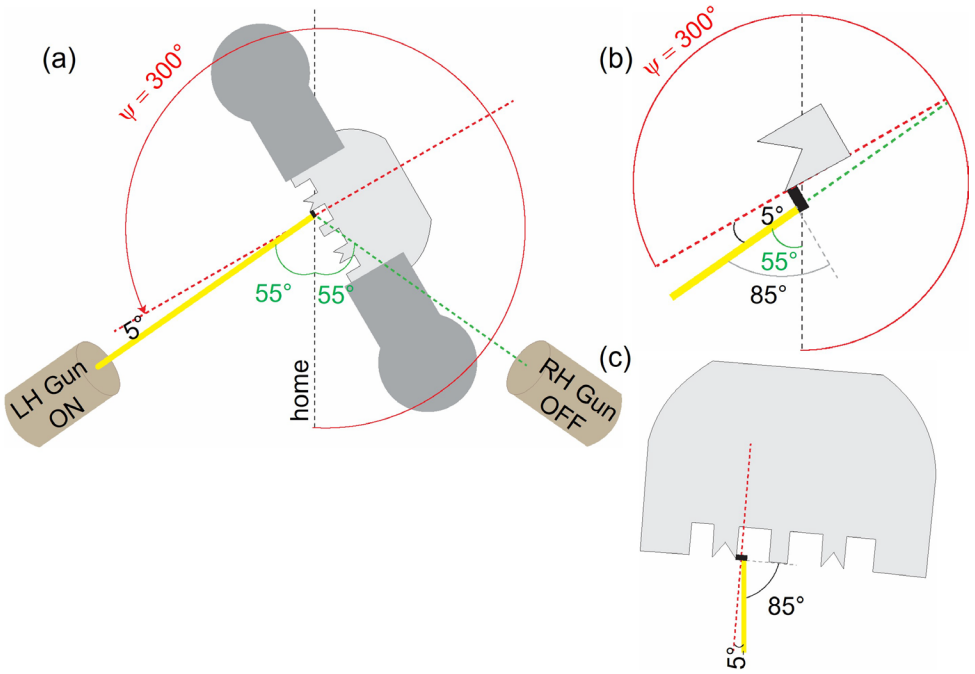

Figure 9. Configuration for using LH gun, sample mounted on right-side face of grid tooth (from perspective of teeth facing down).

Figure 10 presents an optical microscope image of the PIPS interior, illustrating an FIB grid/sample configuration as depicted in Figure 9. In Figure 10a, the red line indicates the direction of the LH gun, while the orange line represents the normal to the sample surface (Ψ = 300°). The sample is milled at a 5° angle from its normal to avoid milling the FIB grid.

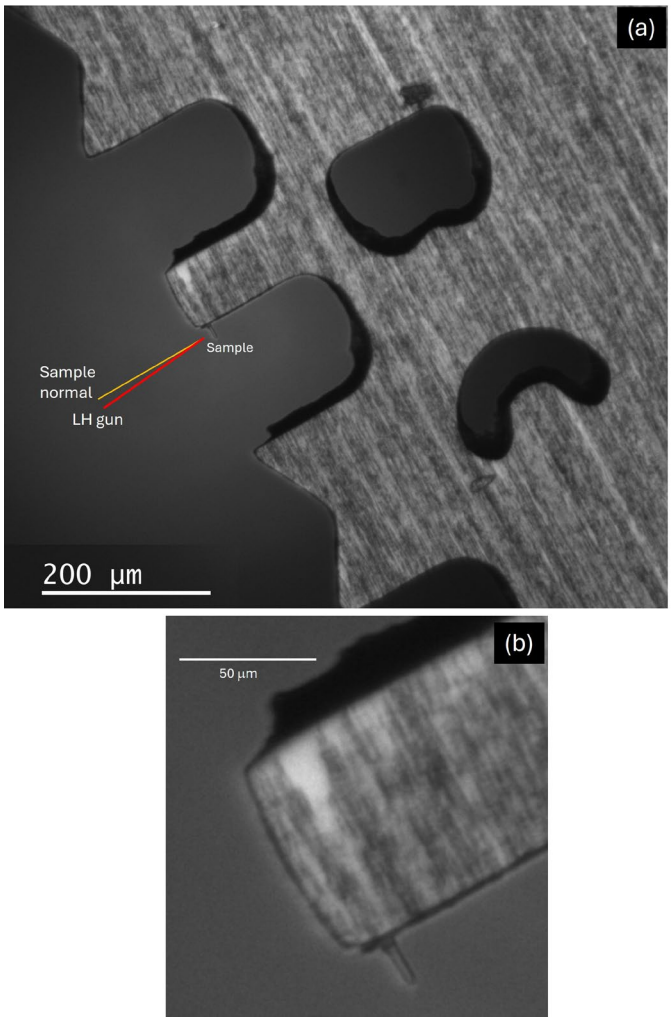

Figure 10. (a) Optical microscope image collected in-situ for the configuration for using left-side gun, sample mounted on right-side face of grid tooth; (b) higher magnification image of the tooth containing the FIB foil.

The i^+ milling angle is set to ±6° relative to the sample plane, with a milling duration of 40 s applied to both sides. Figure 11 illustrates the LH gun positioned at +6°. Rotating the control knob counterclockwise will adjust the angle to –6°. While a combined milling time of 80 s can remove a significant portion of the Pt/C protective layer, an iterative approach—milling and subsequent TEM inspection—is preferred over a single, longer milling cycle. Although this process can be tedious, over-milling and removal of the protective layer is irreversible. For particularly hard or soft samples, adjustments to the milling time, beam energy, and angle may be required.

Figure 11. LH gun set to +6°.

The sample stage resets to the home position once the gun timer expires. To avoid needing to reposition the sample, set the milling time for approximately 1 min, 25 s. Once 40 s have elapsed, change the i^+ gun milling angle from +6 to –6 without interrupting the PIPS milling

3. FIB Samples after Low-Angle Ion Milling

Figure 12 presents an example of a hafnium zirconium oxide (HZO) film grown on a silicon (Si) substrate. Following FIB preparation, the TEM image in Figure 12a reveals a sample sufficiently thin for thickness measurements and low-resolution imaging but inadequate for high-resolution analysis.

We are investigating the relationship between the HZO growth conditions, electrical measurements, and film morphology. As HZO is polymorphic and our target phase is orthorhombic, high-resolution imaging is crucial for visualizing lattice fringes and determining interplanar distances and angles.[6]

Figures 12b–e demonstrate the improvement achieved through low-angle i^+ milling, which enhanced image clarity and revealed distinct crystal morphologies and the Si/HZO interface.

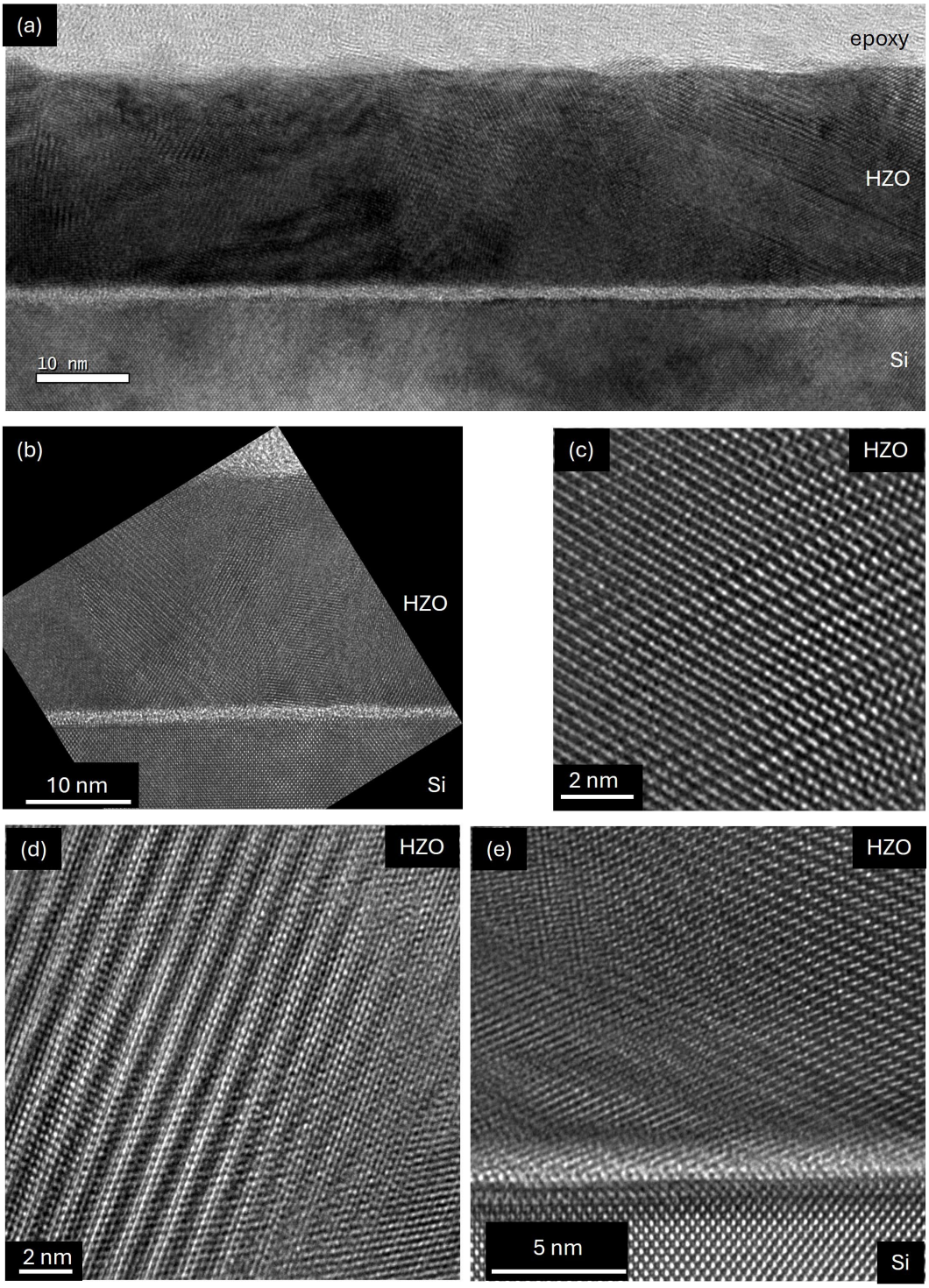

Figure 12. (a) HZO grown on Si, as viewed before low-angle cleanup; (b–e) high-resolution images of HZO on Si from the same sample as view in (a) after a low-angle ion mill cleanup.

In a second example, we examine images collected in STEM mode. Figure 13 shows an aluminum gallium nitride (AlGaN) film on an aluminum nitride (AlN) template. The high-angle annular dark-field (HAADF) image in Figure 13a, acquired after FIB processing, displays compositional oscillations in the AlGaN as vertical stripes—darker bands indicating higher Al content and brighter bands representing lower Al content.[7] Similar to the HZO sample, this material was not initially thin enough for high-resolution imaging.

Figures 13b and 13c present STEM bright- and dark-field images of the AlGaN obtained after a low-angle cleanup. This milling step enabled the resolution of individual nitrogen atoms within the AlGaN structure.

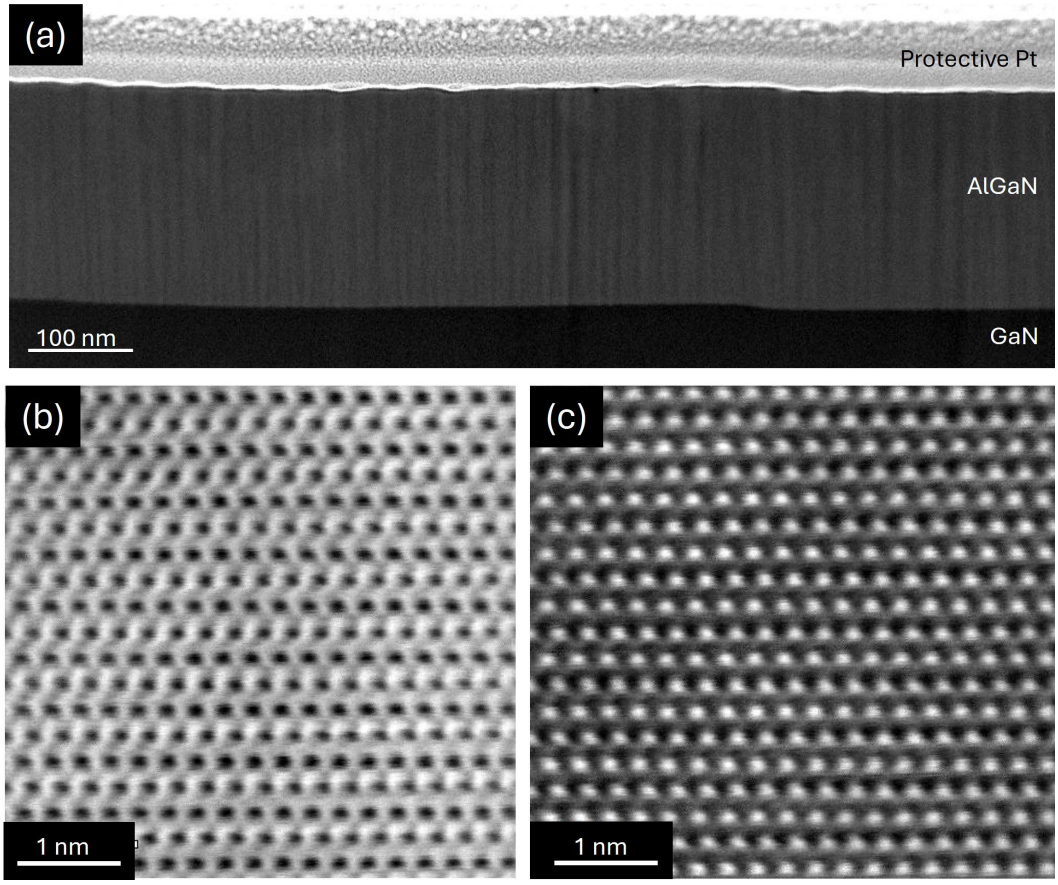

Figure 13. (a) HAADF image of AlGaN on GaN sample before low-angle cleanup. (b) STEM bright-field and (c) STEM dark-field images of the same sample after low-angle cleanup.

4. Conclusion

Low-energy, low-angle Ar^+ milling following FIB preparation enhances the quality of TEM samples. Although FIB techniques can produce sufficiently thin lamellae, final thinning is often limited by challenges in low-energy imaging and the risk of removing protective surface layers. Careful post-FIB treatment in the PIPS allows for controlled, iterative material removal, as demonstrated in HZO and AlGaN samples. This approach improves lattice visibility and interface definition, crucial for advanced materials characterization.

5. References

1. Herbig M, Kumar A. Removal of hydrocarbon contamination and oxide films from atom probe specimens. Microsc Res Tech. 2021;84(2). https://doi.org/10.1002/jemt.23587

2. Gatan, Inc. Argon ion polishing of focused ion beam specimens in PIPS II system. Gatan, Inc.; 2025 [accessed 2024 Mar 25]. https://www.gatan.com/argon-ion-polishing-focused-ion-beam-specimens-pips-ii-system

3. Sarney WL, Leff AC, Hornbuckle BC. Focused-ion beam (FIB) transmission electron microscopy (TEM) sample preparation. DEVCOM Army Research Laboratory (US); 2024. Report No.: ARL-TR-10031.

4. National Center for Biotechnology Information. Periodic table of elements. National Institute for Health (US); 2025 [accessed 2025 Mar 28]. https://pubchem.ncbi.nlm.nih.gov/periodic-table/

5. Kato NI. Reducing focused ion beam damage to transmission electron microscopy samples. J Electron Microsc. 2004:53(5). https://doi.org/10.1093/jmicro/dfh080

6. Sarney WL et al. Monolithic integration and ferroelectric phase evolution of hafnium zirconium oxide in 2D neuromorphic synaptic devices. Mater Today Nano. 2023;24. https://doi.org/10.1016/j.mtnano.2023.100378

7. Sarney WL et al. Formation of spontaneous lateral heterostructures in high Al content AlxGa1−xN alloys grown by high-temperature plasma-assisted molecular beam epitaxy. J Electron Mater. 2024:53(6). https://doi.org/10.1007/s11664-024-10952-x

List of Symbols, Abbreviations, and Acronyms

AlGaN	aluminum gallium nitride
AlN	aluminum nitride
Ar	argon
Ar^+	argon ion
C	carbon
e^-	electron
FIB	focused ion beam
Ga	gallium
Ga^+	gallium ion
GaN	gallium nitride
HAADF	high-angle annular dark field
HZO	hafnium zirconium oxide
i^+	ion
LH	left hand
PIPS	precision ion polishing system
Pt	platinum
RH	right hand
Si	silicon
STEM	scanning transmission electron microscopy
TEM	transmission electron microscopy

1 (PDF)	DEFENSE TECHNICAL INFORMATION CTR DTIC OCA
1 (PDF)	DEVCOM ARL FCDD RLB CI TECH LIB